

Light-Responsive Helical Polypeptides Capable of Reducing Toxicity and Unpacking DNA: Toward Nonviral Gene Delivery**

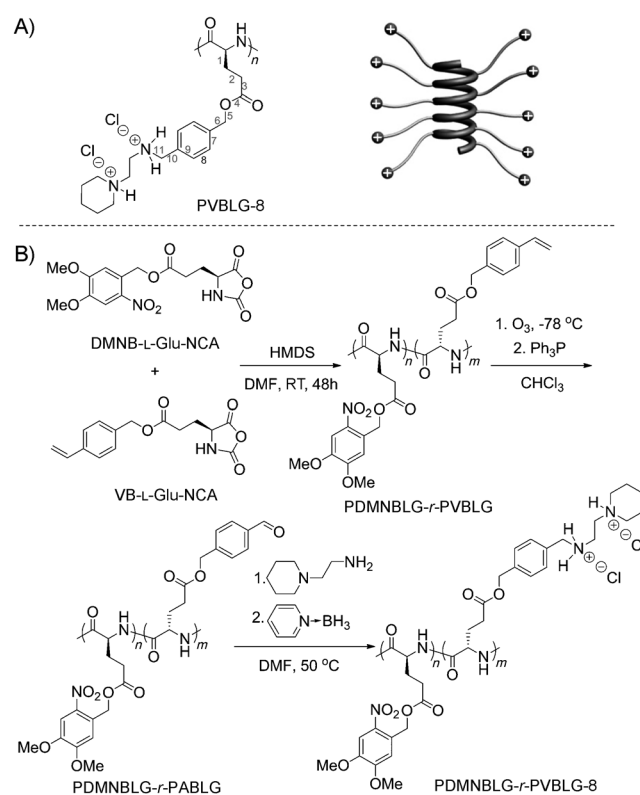
Lichen Yin, Haoyu Tang, Kyung Hoon Kim, Nan Zheng, Ziyuan Song, Nathan P. Gabrielson, Hua Lu, and Jianjun Cheng*

Nonviral gene delivery with synthetic cationic polymeric vectors is widely recognized as an attractive alternative to viral gene delivery, which suffers from inherent immunogenicity and various side effects.^[1] The transfection efficiency and chemotoxicity of these polymeric vectors are often closely related to the density of their cationic charge.^[2] Materials with low charge density usually show low toxicity but are often poor transfection agents. Polycations with high charge density could mediate effective gene transfer, which is however often associated with significant, charge-induced toxicity.^[3] When modified with various charge-reducing moieties, including saccharides,^[4] hydrocarbons,^[5] and poly(ethylene glycol) (PEG),^[6] polycations often benefit from improved safety profiles while in the meantime suffer from significantly reduced gene delivery capabilities. In addition to the charge-induced toxicity, excessive positive charges on polycations would also enhance the electrostatic attraction with the nucleic acids to restrict intracellular gene release.^[3g,7] Therefore, it would be of great interest to develop a highly charged polycation that possesses full transfection capacity and membrane activity during gene transfer, but can be triggered to transform to a less charged or uncharged material with low membrane activity after transfection, such that intracellular DNA unpacking can be facilitated and toxicity can be reduced.^[8]

Cell-penetrating peptides (CPPs), notable for their excellent membrane activities, have been developed and used in drug and gene delivery.^[9] Helical structures are often observed in CPPs or formed in CPPs during membrane transduction, and have been tied to their membrane activity.^[10] Mechanistically, the helical CPP presents a rigid amphiphilic structure that interacts with and destabilizes lipid bilayers, creating transient pathways to facilitate the passive diffusion of exogenous materials.^[9a] Well-known examples of CPPs include oligoarginine, HIV-TAT, and penetratin. Despite their excellent membrane permeability,

CPPs are often too short (10–25 peptide residues) and lack adequate cationic charge to efficiently condense and deliver genes by themselves. As such, CPPs often serve as membrane-active ligands incorporated or conjugated to delivery vehicles to improve delivery efficiencies.^[11]

We recently developed high-molecular-weight (MW), cationic, cell-penetrating, α -helical polypeptides, termed PVBLG-8 (Scheme 1A).^[12] By maintaining a minimum sep-



Scheme 1. A) Schematic illustration of cationic helical PVBLG-8. B) Synthetic route of PDMNBLG-r-PVBLG-8.

aration distance of 11 σ -bonds between the backbone and the side chain charge, the helical structure of PVBLG-8 is stabilized by increased hydrophobic interaction of the side chains and reduced side-chain charge repulsion. Because of the high charge density and higher MW compared to traditional CPPs, PVBLG-8 can condense and deliver DNA to mammalian cells much more effectively, making it a better vector for gene delivery.^[12b] However, PVBLG-8 shows notable cytotoxicity at high concentrations and therefore shares the same concerns as many other polycations. In

[*] Dr. L. Yin,^[†] Dr. H. Tang,^[†] K. H. Kim, N. Zheng, Z. Song, Dr. N. P. Gabrielson, Dr. H. Lu, Prof. Dr. J. Cheng
Department of Materials Science and Engineering
University of Illinois at Urbana-Champaign
1304 W. Green Street, Urbana, IL 61801 (USA)
E-mail: jianjunc@illinois.edu
Homepage: <http://cheng.matse.illinois.edu/>

[†] These authors contributed equally to this work.

[**] J.C. acknowledges support from the NSF (CHE-1153122) and the NIH (NIH Director's New Innovator Award 1DP2OD007246, 1R21EB013379).

Supporting information for this article is available on the WWW under <http://dx.doi.org/10.1002/anie.201302820>.

consistence with previous reports on the correlation between cytotoxicity and helicity of CPPs, the helical structure of PVBLG-8 also contributes to its observed toxicity. Moreover, because of the high density of its cationic charge, PVBLG-8 also suffers from inefficient DNA release. Thus, in attempts to reduce material toxicity as well as facilitate intracellular DNA release, we sought a strategy to reduce both the charge density and the helical content of PVBLG-8 at the post-transfection state. Here, we report the design of cationic α -helical poly(γ -(4,5-dimethoxy-2-nitrobenzyl)-L-glutamate)-*r*-PVBLG-8 (PDMNBLG-*r*-PVBLG-8, Scheme 1B), which maintains high membrane activity during transfection because of high charge density and helical contents, and transforms to a toxicity-reduced and DNA-repelling state with a distorted helix and diminished density of the cationic charge after transfection in response to external triggers.

PVBLG-8 contains stable pendant benzyl ester bonds that are difficult to cleave under physiological conditions, thus prohibiting the conversion of the material into the desired nontoxic, negatively charged, random-coiled poly(glutamic acid). By incorporating various amounts of light-sensitive 4,5-dimethoxy-2-nitrobenzyl-glutamate (DMNBLG) into PVBLG-8 to prepare random PDMNBLG-*r*-PVBLG-8 copolymers, we could enable the photonic manipulation of the toxicity and gene-release profiles of the material after transfection. Because the DMNBLG residues are uncharged and hydrophobic, the polycationic nature and helical structure would be well maintained in PDMNBLG-*r*-PVBLG-8 to exert membrane activity. When a photonic stimulus is applied after transfection, the PDMNBLG domain would yield pendant carboxylate groups (blue segment of the illustration and chemical structure in Figure 1) through light-triggered de-esterification, and the polypeptide would thus have a much reduced density of cationic charge. The intramolecular electrostatic attraction between the negatively charged carboxylate groups and the positively charged amine side groups of the original PVBLG-8 would transform the helical conformation of the parental polypeptide to the helix-disrupted conformation of the light-treated polypeptide. Collectively, the irradiation of PDMNBLG-*r*-PVBLG-8 would lead to a net effect of reducing the cytotoxicity of the material and promoting intracellular gene release (Figure 1). While light-enhanced gene transfection either by charge-switching multivalency^[8a,b] or by supramolecular recognition^[8d] has been reported, the current study provides a novel strategy to modulate the gene transfection and cytotoxicity by regulating the polypeptide helicity.

To test the above-mentioned design, photo-responsive PDMNBLG-*r*-PVBLG-8 with a fixed degree of polymerization of 200 and various molar contents of DMNBLG (10%, 20%, 30%, and 40%, designated as P10, P20, P30, and P40, respectively) were synthesized by ring-opening copolymerization of DMNB-L-Glu-NCA and VB-L-Glu-NCA. Side chains of the resulting PDMNBLG-*r*-PABLG were aminated to yield PDMNBLG-*r*-PVBLG-8 (Scheme 1B). In addition, P0, a nonresponsive control polymer containing no DMNBLG (P0 = PVBLG-8) was also prepared.^[12b] Hexamethyldisilazane (HMDS) as the initiator ensured well-controlled polymerization, evidenced by the monomodal GPC

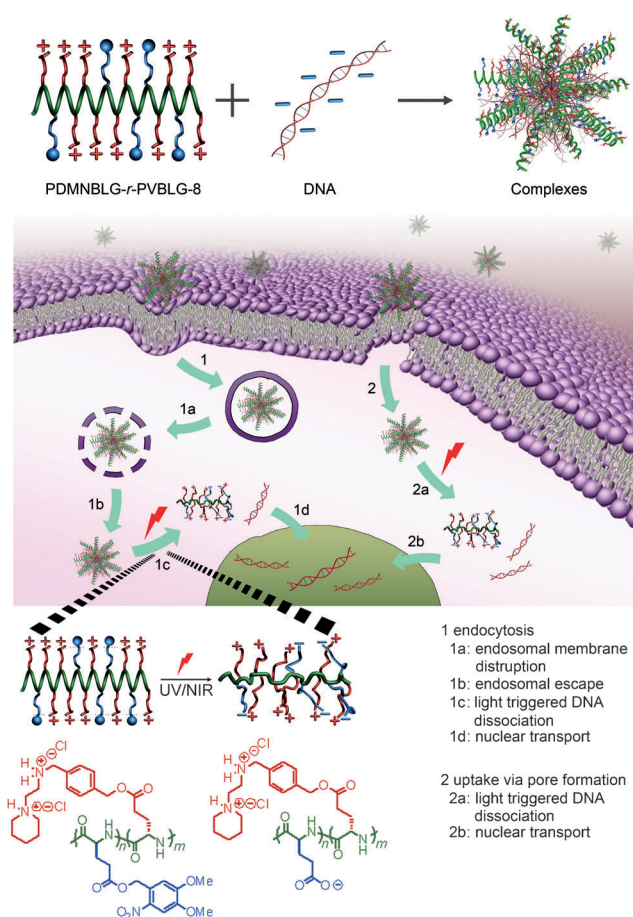


Figure 1. Intracellular kinetics of PDMNBLG-*r*-PVBLG-8/DNA complexes, including uptake by endocytosis and passive diffusion, endosomal escape by membrane destabilization, light-triggered conversion of the charge and secondary structure of the polypeptide, subsequently facilitating intracellular DNA unpacking, and nuclear transport.

curves (Figure S2 in the Supporting Information), well-defined MWs, and the low polydispersity index ($PDI < 1.1$, Table 1).^[13] All synthesized polypeptides exhibited excellent solubility in aqueous solution at $pH < 9$ and adopted α -helical conformations (Figure 2A). The helicities were as high as 90% (Figure S6 in the Supporting Information) and the helical structures were remarkably stable against pH changes between 1 and 9 (Figure 2B), demonstrating that the addition of up to 40 mol% DMNB-L-Glu residues to the random copolymer did not affect the helical conformation of PVBLG-8.

The helicities of PDMNBLG-*r*-PVBLG-8 were demonstrated to be photo-responsive. When an aqueous solution of the polypeptide was irradiated with UV light ($\lambda = 365$ nm, 20 mW cm⁻²), an efficient model light trigger, the absorption at 346 nm in the UV/Vis spectroscopy decreased whereas the absorption at 400 nm increased (Figure S5 in the Supporting Information), indicating cleavage of the photo-labile ester bond and generation of nitrobenzaldehyde.^[14] By plotting the OD₃₄₆ value against the irradiation time, we determined that the photochemical reaction approached maximum conversion after 10 min of irradiation with UV light. UV irradiation also

Table 1: Properties of PDMNBLG-*r*-PVBLG-8.

	M/I ^[a]	M _n (M _n [*]) × 10 ³ ^[b,c]	PDI ^[c]	Composition ^[d]
P0	(200+0)/1	47.7 (49.0)	1.08	PVBLG-8 ₁₉₄
P10	(180+20)/1	47.9 (50.6)	1.02	PDMNBLG ₁₉ - <i>r</i> -PVBLG-8 ₁₇₀
P20	(160+40)/1	57.2 (52.2)	1.02	PDMNBLG ₄₄ - <i>r</i> -PVBLG-8 ₁₇₅
P30	(140+60)/1	55.6 (53.8)	1.03	PDMNBLG ₆₂ - <i>r</i> -PVBLG-8 ₁₄₅
P40	(120+80)/1	52.7 (55.4)	1.06	PDMNBLG ₇₆ - <i>r</i> -PVBLG-8 ₁₁₄

[a] Feed ratio of (DMNB-L-Glu-NCA + VB-L-Glu-NCA)/HMDS.

[b] Obtained MW for PDMNBLG-*r*-PVBLG (expected MW^{*}). [c] Obtained MW and PDI were determined by GPC. [d] The composition was determined by ¹H NMR spectroscopy.

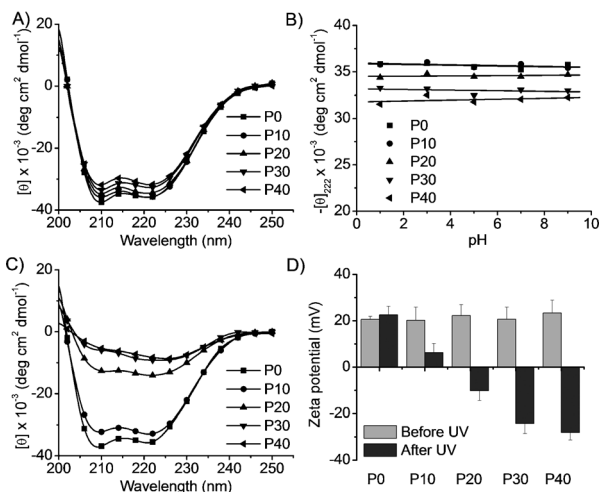


Figure 2. PDMNBLG-*r*-PVBLG-8 with reduced helicity and cationic charge upon UV irradiation (20 mWcm⁻², 10 min). A) CD spectra of PDMNBLG-*r*-PVBLG-8 in water before UV irradiation. B) Helices of PDMNBLG-*r*-PVBLG-8 at different pH values. C) CD spectra of PDMNBLG-*r*-PVBLG-8 in water after irradiation. D) Change of the zeta potential of polypeptide/DNA complexes (N/P ratio = 20) upon UV irradiation.

significantly attenuated the α -helicities of P20, P30, and P40, which contain significant portions of photo-responsive DMNBLG residues, while minimal changes were seen in P0 and P10 (Figure 2C, and Figure S6 in the Supporting Information). The observed helix disruption was attributed to the intramolecular charge attraction between amine groups of PVBLG-8 and carboxylate groups generated through the removal of the DMNB group. The formation of carboxylate groups and the reduction of positive charge of the materials were also supported by the observation that the zeta potentials of all polypeptide/pCMV-Luc/DNA complexes at the optimal N/P (positively charged amine group (N) of each polycation residue/negatively charged phosphate group (P) of each DNA residue) ratio of 20 (diameter of 130–170 nm) were decreased upon UV irradiation (Figure 2D).

P20, which has the highest density of cationic charges among the three PDMNBLG-*r*-PVBLG-8 analogues (P20, P30, and P40) that are susceptible to light-induced helicity reductions (Figure 2C), was selected to study the light-triggered changes of membrane activity and cytotoxicity. Fluorescein isothiocyanate/tris(hydroxymethyl)methane-

thiourea (FITC-Tris, a membrane-impermeable fluorescent dye in the nonreactive form of FITC after reaction of FITC with Tris) was used as a biomarker for membrane pore formation.^[9b] The polypeptides facilitated the uptake of FITC-Tris in HeLa and COS-7 cells by 8–10 fold (Figure 3A),

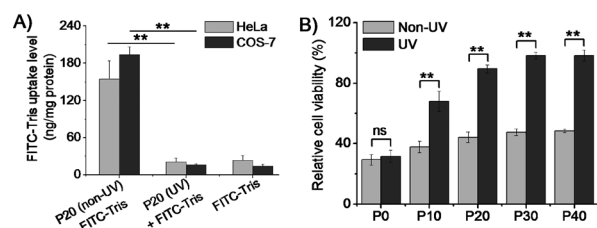


Figure 3. Polypeptides display diminished membrane activity and cytotoxicity upon UV irradiation. A) Uptake of FITC-Tris in HeLa and COS-7 cells in the presence of P20 and UV-treated P20 ($n = 3$). B) Cytotoxicity of polypeptide/DNA complexes in HeLa cells (N/P ratio of 20, 5 μ g DNA/mL) with/without in situ UV irradiation (20 mWcm⁻², 5 min) as assessed by the MTT assay ($n = 3$); ns = no significant difference ($p > 0.05$).

presumably because P20 induced pore formation on cell membranes.^[9b] To validate this hypothesis, FITC-Tris internalization in the presence of UV-pretreated P20 (20 mWcm⁻², 10 min) was studied, showing that light-triggered reduction of the density of cationic charges and loss of α -helicity indeed reduced the membrane activity and pore-formation capability of P20 (P20(UV) + FITC-Tris group vs. P20(non-UV) + FITC-Tris group, $p < 0.05$; $p =$ estimate of the probability that the result has occurred by statistical accident; the lower the p value, the higher the statistical significance). It was therefore not surprising to observe that the cytotoxicities of all photo-responsive polypeptides (P10–P40) were notably reduced upon UV irradiation (Figure S9 in the Supporting Information) as determined by the MTT assay. In a typical experiment in accordance with the transfection process, polypeptide/DNA complexes (N/P ratio of 20) were first incubated with cells for 4 h, followed by UV irradiation for 5 min and further culturing for 20 h before viability assessment (Figure 3B, and Figure S10 in the Supporting Information). Consistently, complexes formed from P10–P40, but not the nonresponsive P0, showed diminished cytotoxicity in response to UV irradiation. These results collectively validated the proposed strategy of eliminating the membrane activity and improving the cell tolerability of polypeptides by post-transfection light exposure. UV light is not biocompatible; but cells that receive low-intensity UV irradiation for a short period of time (20 mWcm⁻², 5 min) showed uncompromised viability ((96.8 \pm 4.2)%, $n = 3$, $n =$ number of experiments), thus indicating that UV irradiation in this proof-of-concept model system did not induce appreciable cytotoxicity that would otherwise jeopardize the analysis of trigger-induced toxicity reduction. The cleaved DMNB also showed minimal toxicity to HeLa cells following 24 h incubation at 0.1 μ molmL⁻¹, corresponding to the concentration of DMNB generated from the UV-irradiated P40/DNA complexes (N/P ratio of 20) at 5 μ gDNA mL⁻¹ during

the transfection process (Figure S11 in the Supporting Information).

We next investigated whether light-triggered alteration of the charge and conformation of the polypeptides would promote intracellular DNA unpacking and gene transfection. As expected, the incorporation of DMNBLG moieties did not compromise the capacity of the polypeptides for DNA delivery, leading to a notable uptake level of YOYO-1-labeled DNA in both HeLa and COS-7 cells as a result of caveolae-mediated endocytosis and energy-independent non-endocytosis (Figure S12 in the Supporting Information). UV-induced DNA release was monitored by the heparin replacement assay.^[15] UV irradiation for 5 min notably facilitated the DNA release from the P20/DNA complexes, leading to almost complete DNA dissociation within 12 h (Figure 4A,

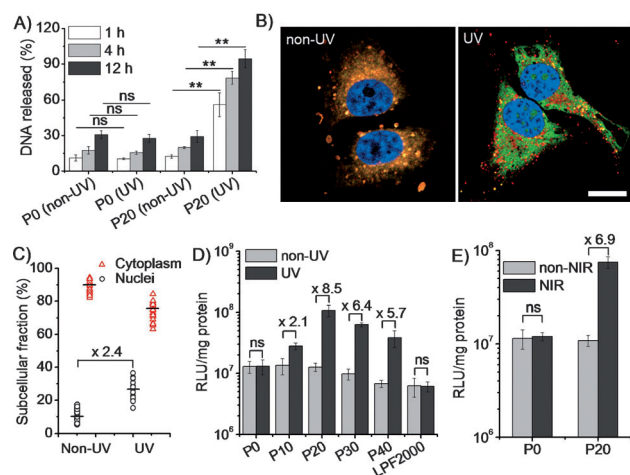


Figure 4. UV (365 nm, 20 mW cm⁻², 5 min)/NIR (750 nm, 3.2 μJ cm⁻²/pulse, 1.5 h) irradiation improves transfection efficiency by facilitating intracellular DNA unpacking and nuclear transport. A) DNA release from nontreated and UV-treated complexes (*n* = 3). B) CLSM images of HeLa cells incubated with RhB-P20 (red)/YOYO-1-DNA (green) complexes with/without UV irradiation (bar = 20 μm). C) Subcellular distribution of YOYO-1-DNA in HeLa cells following treatment with P20/DNA complex and UV irradiation. D) Transfection efficiency in HeLa cells (N/P = 20, 5 μg DNA/mL) with/without UV irradiation (*n* = 3). E) Transfection efficiency of P20/DNA complexes in HeLa cells (N/P = 20, 5 μg DNA/mL) with/without NIR irradiation (*n* = 3). ns = no significant difference (*p* > 0.05).

and Figure S13 in the Supporting Information). Comparatively, UV irradiation exerted no effect on the P0/DNA complexes, confirming that the helix-distorted and cationic-charge-reduced polypeptides promoted DNA unpacking. The size of the complex was markedly augmented upon UV irradiation, consistently signifying reduced DNA condensation by the polypeptides (Figure S8 in the Supporting Information).

Apart from the charge conversion that would facilitate DNA unpacking, we also examined the impact of secondary structure. PVBLG-8 and PVBDLG-8, two homo-polypeptides that possess the same charge density but different conformation (α -helix for PVBLG-8 prepared with L-Glu,

and random-coil for PVBDLG-8 prepared with racemic D,L-Glu^[12b]), were allowed to form complexes with DNA (N/P ratio of 20). PVBLG-8 showed higher DNA condensation than PVBDLG-8 (Figure S14 in the Supporting Information), thus suggesting that the reduction in both charge and helicity in UV-treated PDMNBLG-*r*-PVBLG-8 could synergistically promote the DNA release. By labeling P20 with rhodamine (RhB) and DNA with YOYO-1, we further studied the intracellular DNA unpacking using confocal laser scanning microscopy (CLSM). Compared to nontreated cells, inside which red and green fluorescence were largely overlapped, UV-treated cells exhibited notably enhanced separation of green fluorescence from red fluorescence (Figure 4B), thus suggesting trigger-induced intracellular DNA release. The unpacked DNA spread to the entire cytoplasm and some was localized inside the nuclei (Figure 4B). Since DNA needs to enter the nuclei before it can be transcribed, we further quantified the nuclear distribution of YOYO-1-DNA.^[7] Following the treatment of the cells with the complex for 4 h and subsequent irradiation with UV light, 30% of the internalized DNA was distributed to the nuclei, representing a 2.3-fold increase over nontreated cells (Figure 4C). As a result, UV irradiation led to up to 8.5- and 5.6-fold increase in luciferase expression in HeLa (Figure 4D) and COS-7 cells (Figure S16 in the Supporting Information), respectively. Maximal transfection efficiency was noted for UV-treated P20, outperforming commercial reagent Lipofectamine™ 2000 (LFP2000) by 10–18 fold. The promoted gene transfection of P20/DNA complexes was also noted by flow cytometry when plasmid encoding enhanced green fluorescent protein (pEGFP) was used (Figure S17 in the Supporting Information). UV irradiation did not alter the transfection efficiency of the nonresponsive P0, thus indicating that irradiation itself did not improve gene expression.

Because UV irradiation often suffers from low penetration and potential genotoxic effects when clinically applied, we went on to evaluate the applicability of near-infrared (NIR) modulation in this system. NIR irradiation (750 nm, 3.2 μJ cm⁻²/pulse) eliminated the helicity of P20 (Figure S19 in the Supporting Information), which reached the lowest level following protracted irradiation (1.5 h). In accordance, NIR irradiation for 1.5 h triggered a 6.9-fold increment in the transfection efficiency of P20/DNA complexes in HeLa cells, compared to the unappreciable enhancement of the non-responsive P0/DNA complexes (Figure 4E). As expected, NIR irradiation did not induce cell death (viability of (95.6 ± 6.2)%, *n* = 3). These results validated the potential of regulating the transfection performance of photo-responsive polypeptides using highly penetrating and more biocompatible light. DMNB has negligible absorption in the NIR region, and the slower responsiveness was mainly due to the low two-photon uncaging cross section of the DMNB group.^[14] A more NIR-sensitive Glu-protecting ligand (under development in our group) would substantially enhance the applicability of this class of smart, trigger-responsive, nonviral delivery vectors.

In summary, we developed a class of cationic helical polypeptides with built-in trigger-responsive domains that control the charge and conformational change of the poly-

peptides upon external stimuli. The reduction of cationic charge and helix disruption subsequently resulted in the reduction of membrane activities of the polypeptides and enhancement of the DNA unpacking capacities, thus substantially improving the efficiency of gene delivery with diminished cytotoxicity. As such, one trigger stimulates multiple gene transfection/delivery-relevant changes of material properties, thus provoking desired intracellular responses to overcome various barriers against nonviral gene delivery.

Received: April 5, 2013

Revised: May 25, 2013

Published online: July 5, 2013

Keywords: cell-penetrating peptides · charge conversion · helical structures · nonviral gene delivery

- [1] a) A. K. Salem, P. C. Searson, K. W. Leong, *Nat. Mater.* **2003**, *2*, 668–671; b) K. Roy, H. Q. Mao, S. K. Huang, K. W. Leong, *Nat. Med.* **1999**, *5*, 387–391; c) M. A. Mintzer, E. E. Simanek, *Chem. Rev.* **2009**, *109*, 259–302.
- [2] a) Y. Lee, K. Miyata, M. Oba, T. Ishii, S. Fukushima, M. Han, H. Koyama, N. Nishiyama, K. Kataoka, *Angew. Chem.* **2008**, *120*, 5241–5244; *Angew. Chem. Int. Ed.* **2008**, *47*, 5163–5166; b) K. Miyata, M. Oba, M. Nakanishi, S. Fukushima, Y. Yamasaki, H. Koyama, N. Nishiyama, K. Kataoka, *J. Am. Chem. Soc.* **2008**, *130*, 16287–16294; c) H. M. Liu, H. Wang, W. J. Yang, Y. Y. Cheng, *J. Am. Chem. Soc.* **2012**, *134*, 17680–17687.
- [3] a) B. R. McNaughton, J. J. Cronican, D. B. Thompson, D. R. Liu, *Proc. Natl. Acad. Sci. USA* **2009**, *106*, 6111–6116; b) H. Uchida, K. Miyata, M. Oba, T. Ishii, T. Suma, K. Itaka, N. Nishiyama, K. Kataoka, *J. Am. Chem. Soc.* **2011**, *133*, 15524–15532; c) S. Srinivasachari, K. M. Fichter, T. M. Reineke, *J. Am. Chem. Soc.* **2008**, *130*, 4618–4627; d) H. Wei, J. G. Schellinger, D. S. H. Chu, S. H. Pun, *J. Am. Chem. Soc.* **2012**, *134*, 16554–16557; e) J. Li, C. Yang, H. Z. Li, X. Wang, S. H. Goh, J. L. Ding, D. Y. Wang, K. W. Leong, *Adv. Mater.* **2006**, *18*, 2969–2974; f) J. C. Sunshine, D. Y. Peng, J. J. Green, *Mol. Pharm.* **2012**, *9*, 3375–3383; g) M. S. Shim, Y. J. Kwon, *J. Controlled Release* **2009**, *133*, 206–213; h) J. B. Zhou, J. Liu, C. J. Cheng, T. R. Patel, C. E. Weller, J. M. Piepmeier, Z. Z. Jiang, W. M. Saltzman, *Nat. Mater.* **2012**, *11*, 82–90.
- [4] P. M. McLendon, K. M. Fichter, T. M. Reineke, *Mol. Pharm.* **2010**, *7*, 738–750.
- [5] D. F. Zhi, S. B. Zhang, B. Wang, Y. N. Zhao, B. L. Yang, S. J. Yu, *Bioconjugate Chem.* **2010**, *21*, 563–577.
- [6] S. Takae, K. Miyata, M. Oba, T. Ishii, N. Nishiyama, K. Itaka, Y. Yamasaki, H. Koyama, K. Kataoka, *J. Am. Chem. Soc.* **2008**, *130*, 6001–6009.
- [7] X. Zhao, L. Yin, J. Ding, C. Tang, S. Gu, C. Yin, Y. Mao, *J. Controlled Release* **2010**, *144*, 46–54.
- [8] a) M. A. Kostianen, D. K. Smith, O. Ikkala, *Angew. Chem.* **2007**, *119*, 7744–7748; *Angew. Chem. Int. Ed.* **2007**, *46*, 7600–7604; b) G. Han, C. C. You, B. J. Kim, R. S. Turingan, N. S. Forbes, C. T. Martin, V. M. Rotello, *Angew. Chem.* **2006**, *118*, 3237–3241; *Angew. Chem. Int. Ed.* **2006**, *45*, 3165–3169; c) X. A. Jiang, Y. R. Zheng, H. H. Chen, K. W. Leong, T. H. Wang, H. Q. Mao, *Adv. Mater.* **2010**, *22*, 2556–2560; d) S. K. M. Nalluri, J. Voskuhl, J. B. Bultema, E. J. Boekema, B. J. Ravoo, *Angew. Chem.* **2011**, *123*, 9921–9925; *Angew. Chem. Int. Ed.* **2011**, *50*, 9747–9751; e) X. H. Liu, J. W. Yang, D. M. Lynn, *Biomacromolecules* **2008**, *9*, 2063–2071.
- [9] a) K. M. Stewart, K. L. Horton, S. O. Kelley, *Org. Biomol. Chem.* **2008**, *6*, 2242–2255; b) G. Ter-Avetisyan, G. Tuenne-mann, D. Nowak, M. Nitschke, A. Herrmann, M. Drab, M. C. Cardoso, *J. Biol. Chem.* **2008**, *284*, 3370–3378.
- [10] a) P. Ruzza, A. Calderan, A. Guiotto, A. Osler, G. Borin, *J. Pept. Sci.* **2004**, *10*, 423–426; b) D. S. Daniels, A. Schepartz, *J. Am. Chem. Soc.* **2007**, *129*, 14578–14579.
- [11] a) R. N. Johnson, D. S. H. Chu, J. Shi, J. G. Schellinger, P. M. Carlson, S. H. Pun, *J. Controlled Release* **2011**, *155*, 303–311; b) M. Meyer, A. Philipp, R. Oskuee, C. Schmidt, E. Wagner, *J. Am. Chem. Soc.* **2008**, *130*, 3272–3274.
- [12] a) H. Lu, J. Wang, Y. G. Bai, J. W. Lang, S. Y. Liu, Y. Lin, J. J. Cheng, *Nat. Commun.* **2011**, *2*, 206; b) N. P. Gabrielson, H. Lu, L. C. Yin, D. Li, F. Wang, J. J. Cheng, *Angew. Chem.* **2012**, *124*, 1169–1173; *Angew. Chem. Int. Ed.* **2012**, *51*, 1143–1147.
- [13] H. Lu, J. J. Cheng, *J. Am. Chem. Soc.* **2007**, *129*, 14114–14115.
- [14] N. Fomina, C. McFearin, M. Sermsakdi, O. Edigin, A. Almutairi, *J. Am. Chem. Soc.* **2010**, *132*, 9540–9542.
- [15] W. Y. Seow, Y. Y. Yang, A. J. T. George, *Nucleic Acids Res.* **2009**, *37*, 6276–6289.